

# Optimal Location of FACTS for Voltage stability using Modified Particle Swarm Optimization

Whei-Min Lin, *Member, IEEE*, Kai-Hung Lu, Chih-Ming Hong and Chia-Sheng Tu

**Abstract**—Voltage security is a crucial issue in power systems especially under heavily loaded condition. In the new scheme of restructuring, voltage stability problem becomes even more serious. In order to solve the kind of thorny problem, experts employ various methods for relieving congested difficulties. There are many new power-electronics-based devices using to solve the difficult problems recently. Unified Power Flow Controller (UPFC) is the most powerful device of these devices. A new model is proposed in this thesis to improve existing power-based model by using the Norton Equivalent Theorem. The proposed model can be integrated with the Equivalent Current Injection (ECI) power flow model easily. By ECI algorithm, it is much quickly and precisely to implement power flow calculations. By making use of modified particle swarm optimization (MPSO), the optimal location of UPFC in power system will be obtained. Finally simulation shows the optimal location and capacity of new UPFC with ECI model to enhance power system voltage stability by using MPSO. The proposed method demonstrates the improvement of voltage stability margin.

**Keywords**—Modified particle swarm optimization (MPSO), voltage stability, Unified Power Flow Controller (UPFC), Equivalent -Current-Injection (ECI)

## I. INTRODUCTION

Power systems components mainly consist of generators, transmission lines, transformers, switches, active or passive compensators and loads. Power system networks are complex systems that are nonlinear, non-stationary, and prone to disturbances and faults. Reinforcement of a power system can be accomplished by improving the voltage profile, increasing the transmission capacity and others. Flexible AC Transmission System (FACTS) devices are an alternate solution to address some of those problems [1][5].

The FACTS devices can be categorized into three types, such as series controllers, shunt controllers and combined series-shunt controllers. In principle, the series controllers inject voltage in series with the line and the shunt controllers inject current into the system at the point of connection. The combined series-shunt controllers inject current into the system with the shunt part of the controllers and voltage in series in the line with the series part of the controllers.

In the case of voltage support, shunt FACTS devices, such as STATCOM and SVC are typically used [2-3]. This study is focused on the steady state performance of multiple

UPFC devices in the power system. Particularly, it is desired to determine their optimal location and capacity.

Traditional optimization methods such as mixed integer linear and non linear programming have been investigated to address this issue; however difficulties arise due to multiple local minima and overwhelming computational effort. In order to overcome these problems, Evolutionary Computation Techniques have been employed to solve the optimal allocation of FACTS devices.

This paper applied the ability of the modified particle swarm optimization (MPSO) efficiency. The objective of MPSO is to improve the searching quality of ants by optimizing themselves to generate a better result. This method can not only enhance the neighborhood search, but can also search the optimum solution quickly to advance convergence.

The load flow analysis (commonly called load flow or power flow) is the basic tool for investigating power system state variables, and it is very important part of the system supervisory, planning and optimal operation. The unbalance three-phase load flows based on the Equivalent-Current-Inject (ECI) were applied successfully to the distribution system [4][7][8]. It is unable to apply the ECI model to the high voltage transmission systems, because of the voltage – controlled buses (PV Bus). In this a new power flow approach based on ECI model and Cartesian coordination is presented. PV Bus model were developed, and according to the network characteristics, the decoupled models were also proposed.

This paper introduces the application of MPSO for optimal location and capacity of a new UPFC with ECI model in the power system. It is organized as follows: Section II UPFC with ECI. Section III presents the basic concepts of modified particle swarm optimization (MPSO). In section IV the objective function to be optimized is described. In section V simulation results are presented. In section VI conclusions and future work are given.

## II. UPFC WITH ECI MODEL

### A. UPFC Basic Concept

The Fig. 1 shows a conceptual representation of UPFC in a two-machine power system. In Fig. 1, the series branch of UPFC is modeled as a generalized synchronous voltage, and represented at the power system frequency by voltage phasor,  $V_{CR}$ , and its phase angle,  $\rho$ , in series with the transmission line. Therefore, it is clear that the effective sending end voltage is modified by the UPFC series injected voltage in both magnitude and its phase angle, and as a result it is able to control, by adjusting the magnitude and the phase of  $V_{CR}$ , the transmittable active power as well as the reactive power. Moreover, in dynamic control applications, it is also able to provide power oscillation damping by real-time modulating

The Authors are with the Department of Electrical Engineering, National Sun Yat-Sen University, Kaohsiung 80424, Taiwan. (e-mail: D953010011@student.nsysu.edu.tw).

the real power of the ac system. This is the result of its ability to alternatively insert a virtual positive and negative damping resistor in series with the line in accordance with the angular acceleration and deceleration of the disturbed generators.

In practical hardware implementations, the UPFC consists of two voltage sourced converters, as illustrated in Fig. 1. The two back-to-back converters, as labeled “Shunt Converter” and “Series Converter” in the figure are designed to be operated from a common DC link voltage supported by a DC storage capacitor. In normal operations, the phase angle of the series voltage can be chosen independently of the line current between 0 and  $2\pi$ , and its magnitude can be varied between zero and a pre-specified maximum value. Therefore the real power can freely flow in either direction between the AC terminals of the two converters and each converter can also generate or absorb reactive power independently at its own AC output terminals to affect system voltages.

In the UPFC system, Series Converter, the series branch, operated as a SSSC, is used to perform the main control functions of a UPFC. It generates voltage,  $V_{CR}$ , at the system frequency controlled by a proper switching control technique. During the operation the voltage,  $V_{CR}$ , is added to the AC system terminal voltage,  $V_k$ , by the series connected injection series transformer,  $T_{se}$ . The transmission line current flows through this voltage source resulting in reactive and active power exchange between it and the ac system. The reactive power exchanged at the ac terminal is generated internally by the converter. The active power exchanged at the ac terminal is converted into dc power which appears at the dc link as a positive or negative active power demand.

Shunt Converter connected in shunt with the AC power system via a shunt transformer,  $T_{sh}$ , operated as a STATCOM, is used primarily to provide the real power demand of series converter at the common DC link terminal from the AC power system. Since shunt converter can also generate or absorb reactive power at its AC terminal, independently of the real power transferred to (or from) the DC terminal. It follows that, with proper controls, it can also fulfill the function of an independent STATCOM operations providing reactive power compensation for the transmission line and thus executing an indirect voltage regulation at the input terminal of the UPFC. It is important to note that there is a closed direct path for the active power negotiated by the action of series voltage injection through two converters back to the line, the corresponding reactive power exchanged is supplied or absorbed locally by series converter and therefore doesn't have to be transmitted by the line. Thus, shunt converter can be operated at a unity power factor or controlled to have a reactive power exchange with the line independent of the reactive power exchanged by converter 2. Obviously, there is no reactive power flow through the UPFC dc link. In addition, the UPFC has the flexibility the control either its series or shunt branch or both to achieve a desired effect on the power flow transmitted between two buses.

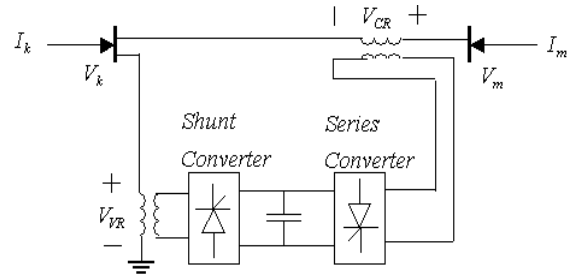


Fig. 1. UPFC connected to power system

The UPFC active  $P_m$  and reactive power  $Q_m$  are shown in (1) and (2).

$$P_m = \frac{(V_k + V_{CR}) \cdot V_m \sin \delta}{X} \quad (1)$$

$$Q_m = \frac{(V_k + V_{CR}) \cdot V_R}{X} (1 - \cos \delta) \quad (2)$$

where  $X$ : is coupling transformer equivalent reactance.

$$\delta: \theta_k - \theta_m$$

In voltage control mode, the reactive current is automatically regulated to maintain the transmission line voltage at the point of connection to a reference value, with a defined droop characteristic. The droop factor defines the per unit voltage error per unit of reactive current within the current range of the converter. The convert supplies leading current to the AC system if the converter output voltage  $V_{sh}$  is made to lead the corresponding AC system voltage  $V_k$ . Then it supplies reactive power to the AC system by capacitive operation. Conversely, the converter absorbs lagging current from the AC system; if the converter output voltage  $V_{sh}$  is made to lag the AC system voltage  $V_k$  then it absorbs reactive power to the AC system by inductive operation. If the output voltage is equal to the AC system voltage, the reactive power exchanges.

### B. UPFC with ECI

The UPFC can act as on equivalent voltage source series reactance. Voltage source can transform the current source by way of Norton Theorem of the  $\pi$ -circuit as shown in Fig. 2. It is important to note that there is a closed direct path for the active power negotiated by the action of series voltage injection through converter 1 and 2 back to the line.

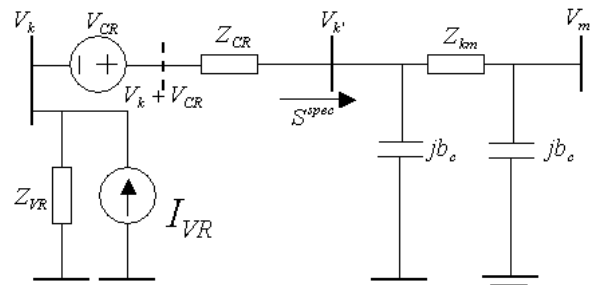


Fig. 2 Transmission line equivalent model UPFC equivalent circuit diagram

According to Fig. 2 with ECI model inferential reasoning as follows in equations.

$$I_{VR} = V_{VR} / Z_{VR} \quad (3)$$

That is the device does not generate or absorb active power internally. This constraint can be stated as:

$$P_{CR} = P_{VR} \quad (4)$$

$$\begin{aligned}
 S_{VR} &= V_k I^* \\
 &= V_k \left( \frac{V_k - V_{VR}}{Z_{VR}} \right)^* \\
 &= \frac{|V_k|^2}{Z_{VR}^*} - V_k \left( \frac{V_{VR}}{Z_{VR}} \right)^* \\
 &= \frac{|V_k|^2}{Z_{VR}^*} - V_k I_{VR}^*
 \end{aligned} \tag{5}$$

where  $I_{VR}$ : shunt branch current

$V_{VR}$ : shunt branch voltage

$Z_{VR}$ : shunt branch impedance equals  $R_{VR} + jX_{VR}$

$P_{CR}, P_{VR}$ : are the active powers supplied or absorbed in the series and shunt converters respectively.

According to the Newton-Raphson algorithm [4], the ECI mismatch equation with UPFC model can be written a new admittance matrix as

$$I_{k,k'} = S^{spec} / V_{k'} \tag{6}$$

$$I_{k,k'} = (V_k + V_{CR} - V_{k'}) \cdot (g_{CR} + jb_{CR}) \tag{7}$$

$$I = Y_{matrix}^{new} V \tag{8}$$

$$\begin{bmatrix} \vdots \\ I_k \\ \vdots \\ I_{k'} \\ \vdots \\ I_{k,k'} \end{bmatrix} = \begin{bmatrix} \dots & \dots & \dots & \dots & \dots & \dots \\ \dots & \dots & \dots & \dots & \dots & g_{CR} + jb_{CR} \\ \dots & \dots & \dots & \dots & \dots & \vdots \\ \dots & \dots & \dots & \dots & \dots & -g_{CR} - jb_{CR} \\ \dots & \dots & \dots & \dots & \dots & \vdots \\ 0 & g_{CR} + jb_{CR} & 0 & -g_{CR} - jb_{CR} & 0 & g_{CR} + jb_{CR} \end{bmatrix} \begin{bmatrix} \vdots \\ V_k \\ \vdots \\ V_{k'} \\ \vdots \\ V_{CR} \end{bmatrix} \tag{9}$$

where  $g_{CR} + jb_{CR} = 1/(Z_{CR})$ ,  $S^{spec}$  is the specified constant apparent power,  $Y_G^{new} = \text{Re}(Y_{matrix}^{new})$ ,  $Y_B^{new} = \text{Im}(Y_{matrix}^{new})$ .

### III. MODIFIED PARTICLE SWARM OPTIMIZATION

#### A. Basic PSO

PSO, as a population-based algorithm, exploits a population of individuals to probe promising regions of the search space. The population is called a swarm and the individuals, particles. As the swarm iterates, the fitness of the global best solution improves (decreases for minimization problem). It is expected to happen that all particles being influenced by the global best eventually approach the global best. If the fitness does not improve despite however many runs the PSO is iterated, then convergence has been achieved. In the pioneering work of Kennedy and Eberhart in 1995, the particle position and velocity is defined by [9]:

$$\begin{aligned}
 V_{[i],[j]}^{k+1} &= V_{[i],[j]}^k + C_1 \cdot rand_1 \cdot (X\_Lbest_{[i],[j]}^k - X_{[i],[j]}^k) \\
 &+ C_2 \cdot rand_2 \cdot (X\_Gbest_{[i],[j]}^k - X_{[i],[j]}^k)
 \end{aligned} \tag{10}$$

$$X_{[i],[j]}^{k+1} = X_{[i],[j]}^k + V_{[i],[j]}^{k+1}$$

where:

$[i],[j]$ : Population number and particles number.

$V_{[i],[j]}^k$ : Velocity of the particle in the  $k_{th}$  iteration.

$X_{[i],[j]}^k$ : Position of the particle in the  $k_{th}$  iteration.

$X\_Lbest_{[i],[j]}^k$ :  $I_{th}$  fitness best in the  $k_{th}$  iteration.

$X\_Gbest_{[i],[j]}^k$ : Population global best in the  $k_{th}$  iteration.

$C_1, C_2$ : Cognitive and Social component, respectively: they influence how much the particle's personal best and

the global best (respectively) influence its movements.

$rand_1, rand_2$ : Uniform random numbers between 0 and 1.

#### B. Modified PSO

A weight factor,  $\omega_k$ , was added to the previous velocity of the particle. This allows control on the mechanism responsible for the velocities magnitude, which fosters the danger of swarm explosion and divergence, or fast convergence and being trapped in local minima. Thus, equation (10) can be re-written including the weight factor,  $\omega_k$ .

$$\begin{aligned}
 V_{[i],[j]}^{k+1} &= \omega_k * V_{[i],[j]}^k + C_1 \cdot rand_1 \cdot (X\_Lbest_{[i],[j]}^k - X_{[i],[j]}^k) \\
 &+ C_2 \cdot rand_2 \cdot (X\_Gbest_{[i],[j]}^k - X_{[i],[j]}^k)
 \end{aligned} \tag{11}$$

$$X_{[i],[j]}^{k+1} = X_{[i],[j]}^k + V_{[i],[j]}^{k+1}$$

The second challenge is to find a feasible weight factor that prevents prematurely because it affects the convergence and the ability of the swarm to find the optimum. A suitable value of  $\omega_k$  provides the desired balance between the global and local exploration ability of the swarm and, consequently, improves the effectiveness of the algorithm. At the beginning, a large inertial weight is better because it gives priority to global exploration of the search space. It can be gradually decreased so as to obtain refined solutions. To introduce chaotic behavior, the iterator called Logistic Map is defined by the following equation:

$$f_k = \mu \cdot f_{k-1} (1 - f_{k-1}) \tag{12}$$

Where  $\mu$  is a control parameter and has a real value between 0 and 4. Despite the apparent simplicity of the equation, the solution exhibits a rich variety of behaviors. The value of  $\mu$  determines whether  $f_k$  stabilizes at a constant size, oscillates between a limited sequence of sizes, or behaves chaotically in an unpredictable pattern. And also the behavior of the system is sensitive to initial values of  $f_k$ . Equation (12) displays chaotic dynamics when  $\mu=4.0$  and  $f_0 \notin \{0, 0.25, 0.5, 0.75, 1.0\}$  [18]. After some tests, the value chosen for  $\omega_0, \mu$  and  $f_0$  are 3.5, 4.0 and 0.65, respectively. Therefore, the weight inertial factor is calculated in every  $k_{th}$  iteration as:

$$\omega_k = \left\{ \frac{\omega_0}{1 + (\log k)^2} \right\} \cdot (f_k) \tag{13}$$

### IV. OBJECTIVE FUNCTION

In such a power network, it is desirable to keep the voltage deviations between  $\pm 5\%$  to avoid voltage collapses during faulty conditions. In general, if the load requirements increase, the voltages at the corresponding buses may drop below 0.95p.u. and consequently an additional voltage support is needed at that particular bus. In this study, the voltage support will be provided by a UPFC with ECI model, and its optimal location and capacity will be determined by using MPSO.

For instance, the IEEE 30-Bus system in Fig. 4 has 5 generators buses where voltage is regulated by the generator AVRs. These generator buses do not need a UPFC and are omitted from the MPSO search process. Also considering the topology of the system, the bus numbers are limited to the range from 1 to 30.

A. UPFC selection to install the location principle

1. Because UPFC are expensive, therefore the minimum device installed is searched for economic efficiency reasons.
2. Generator buses where voltages are regulated by the generator do not need UPFC installation.
3. Each bus is limited to the installation of one device. Installing more does not represent a significant effect.
4. If the bus voltage is above 0.95 p.u., then UPFC is not installed.

According to the above discussion, candidates Bus are shown in Table I.

TABLE I  
CANDIDATE BUS

Bus	15	18	19	20	21	22	23
Bus	24	25	26	27	28	29	30

B. Objective function:

The objective function of optimized power flow is to reduce cost of electricity as below:

$$\text{Mim } F(P_{Gi}) = \sum_{i=1}^{N_G} a_i P_{Gi}^2 + b_i P_{Gi} + c \quad (14)$$

where the system constraints could compose of power balance constraints and inequation constraint.

i) power balance constraints:

$$\begin{cases} -I_r^{\text{spec}} + I_r^{\text{cal}} = 0 \\ -I_i^{\text{spec}} + I_i^{\text{cal}} = 0 \\ -P_G + P_{\text{Load}} + P^{\text{cal}} = 0 \\ -|V_G|^2 + |V^{\text{cal}}|^2 = 0 \end{cases} \quad (15)$$

ii) inequation constraint:

$$\begin{cases} S_{ij}^2 \leq \bar{S}_{L,ij}^2 \\ S_{ji}^2 \leq \bar{S}_{L,ji}^2 \\ P_{Gi} \leq P_{Gi} \leq \bar{P}_{Gi} \\ |V_i|^2 \leq (e_i^2 + f_i^2) \leq |V_i^{\text{cal}}|^2 \\ V_{Shm} \leq V_{Shm} \leq \bar{V}_{Shm} \\ \theta_{Shm} \leq \theta_{Shm} \leq \bar{\theta}_{Shm} \\ V_{Sem} \leq V_{Sem} \leq \bar{V}_{Sem} \\ \theta_{Sem} \leq \theta_{Sem} \leq \bar{\theta}_{Sem} \end{cases} \quad (16)$$

where

$a_i, b_i, c_i$ : fuel cost coefficients of thermal plant

$|V_i|$ : voltage magnitude at bus i

$e_i, f_i$ : Real and imaginary part of voltage  $V_i$  at bus i

$P_{Gi}$ : Dispatchable active power at bus i

$(i, j)$ : Transmission line connecting buses i and j

$S_{ij}^2, S_{ji}^2$ : Apparent power of transmission line (i,j) or (j,i)

$\bar{S}_{L,ij}^2, \bar{S}_{L,ji}^2$ : Apparent power limit of transmission line (i,j) or (j,i), where  $\bar{S}_{L,ij}^2 = \bar{S}_{L,ji}^2$ .

$V_{shm}$ : The shunt voltage of UPFC  $V_s$  at candidate bus m

$\theta_{shm}$ : The shunt phase angle of UPFC at candidate bus m

$V_{sem}$ : The series voltage of UPFC  $V_s$  at candidate bus m

$\theta_{sem}$ : The series phase angle of UPFC at candidate bus m

V. SIMULATION RESULTS

A 30-Bus test system as shown in Fig. 3 is used for this paper. The test system consists of 5 generators and 24 PQ bus (or load bus). The simulation is run in MATLAB.

The problem to be addressed consists of finding the optimal location (bus number) and power rating (MVA) of STATCOM with ECI model. In this case the MPSO is able to find different options for both location and capacity of the STATCOM with the ECI model.

The solution found by MPSO, in terms of bus location and capacity for each MPSO unit, is shown in Table II.

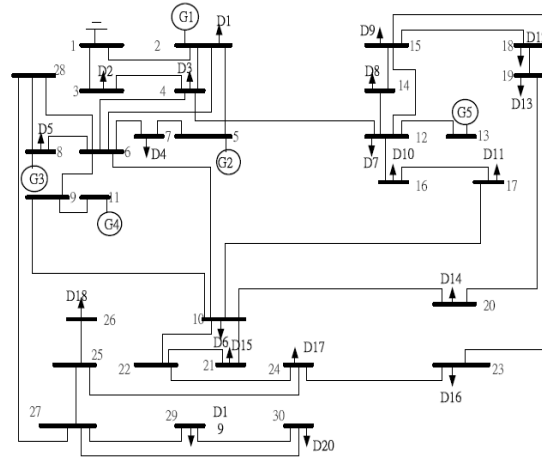


Fig. 3 The 30-bus test system

TABLE II  
SOLUTION FOUND BY MPSO

STATCOM Unit	Location (Bus number)	Capacity (MVA)
1	18	51.613
2	27	24.165

The best solution is found by inserting UPFC at bus 18 and bus 27. The power flow results, the voltage comparison with and without UPFC is show in Fig. 5 and Table III and IV. Table V show the comparison of MPSO, GA and EP. The system without the UPFC has 17 buses with voltage below 0.95 p.u.. Once the UPFC units are connected to buses 18 and 27 the voltage is improved.

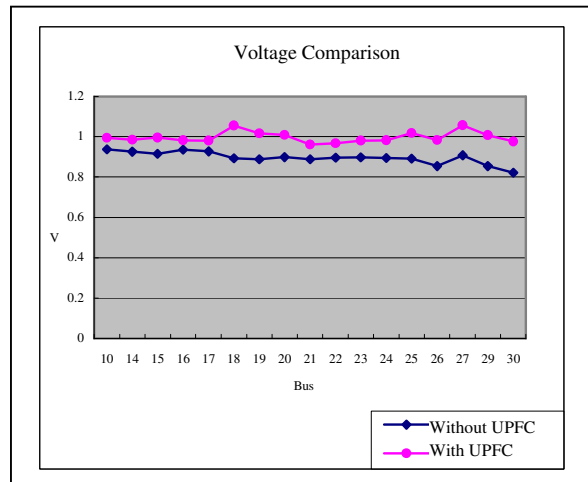


Fig.4 Voltage comparison

TABLE III  
BUS VOLTAGE FROM POWER FLOW RESULT

Bus number	Voltage p.u. w/o UPFC units	Voltage p.u. with UPFC units
10	0.93760	<b>0.99402</b>
14	0.92612	<b>0.98576</b>
15	0.91577	<b>0.99541</b>
16	0.93683	<b>0.98307</b>
17	0.92725	<b>0.98056</b>
18	0.89363	<b>1.05500</b>
19	0.88846	<b>1.01710</b>
20	0.89860	<b>1.00930</b>
21	0.88873	<b>0.96099</b>
22	0.89516	<b>0.96705</b>
23	0.89802	<b>0.98157</b>
24	0.89414	<b>0.98194</b>
25	0.89148	<b>1.01800</b>
26	0.85369	<b>0.98311</b>
27	0.90785	<b>1.05700</b>
29	0.85377	<b>1.00760</b>
30	0.82140	<b>0.97714</b>

TABLE IV  
POWER FLOW RESULT BY ECI WITH UPFC

Branch		P_Flow	Q_Flow	Branch		P_Flow	Q_Flow
From	To	(pu.)	(pu.)	From	To	(pu.)	(pu.)
1	2	<b>-0.68044</b>	0.2175	12	13	<b>-0.79467</b>	0.04432
1	2	<b>-0.35116</b>	0.09517	12	14	<b>0.79103</b>	-0.2374
1	3	<b>0.27365</b>	-0.02928	12	15	<b>-0.08746</b>	0.0434
2	4	<b>0.44589</b>	-0.07865	12	16	<b>-0.08118</b>	0.13026
2	5	<b>-0.25223</b>	0.04623	14	15	<b>0.54618</b>	-0.4507
2	6	<b>0.33446</b>	-0.11717	15	18	<b>-0.10062</b>	0.10531
3	4	<b>0.19825</b>	-0.01425	15	23	<b>-0.30458</b>	-0.09909
4	6	<b>-0.4522</b>	-0.14921	16	17	<b>-0.17958</b>	0.11009
4	12	<b>0.85641</b>	0.05011	18	19	<b>-0.10317</b>	0.0917
5	7	<b>0.56868</b>	-0.13327	19	20	<b>-0.10541</b>	0.05531
6	7	<b>-0.46065</b>	0.26751	21	22	<b>0.16808</b>	-0.04415
6	8	<b>-0.56931</b>	0.16616	22	24	<b>-0.35057</b>	-0.04888
6	9	<b>-0.04684</b>	0.00025	23	24	<b>0.24557</b>	0.00232
6	10	<b>0.83892</b>	0.17528	24	25	<b>-0.12804</b>	0.05317
6	28	<b>0.10794</b>	0.00889	25	26	<b>0.10838</b>	0.02611
8	28	<b>0.1504</b>	-0.05301	25	27	<b>-0.24029</b>	0.0203
9	10	<b>0.88214</b>	0.37872	27	29	<b>0.39985</b>	-0.02452
9	11	<b>-0.90104</b>	0.08518	27	30	<b>-0.28094</b>	0.27535
10	20	<b>0.10741</b>	-0.04443	28	27	<b>0.25664</b>	0.00609
10	21	<b>0.17221</b>	0.09721	29	30	<b>0.36615</b>	-0.09617
10	22	<b>0.91412</b>	0.09331				

TABLE V  
ITERATIONS AND CPU TIMES BY MPSO

		MPSO	GA	EP
Time(s)	Max_time(s)	<b>869</b>	712	1169
	Min_time(s)	<b>95</b>	51	122
	Avg_time(s)	<b>420</b>	583	506
	CPUtime/count	<b>18.4</b>	18.33	16.96
Cost (\$/h)	Worst	<b>774.7703</b>	774.8686	775.5145
	Best	<b>774.7575</b>	774.7575	774.7575
	Average	<b>774.7580</b>	774.7600	774.7732
Count	Max_count	<b>44</b>	39	69
	Min_count	<b>4</b>	2	6
	Avg_count	<b>23.14</b>	31.82	29.86

Additionally, In order to study the effect of the load conditions in the optimal solution found by the MPSO, simulations are carried out by changing the load in each load

center in a range from 30% to 90%.

The Fig. 5 and Fig. 6 are the with and without UPFC voltage comparison for different load. In Fig. 6 and Fig. 7 is registered again a voltage improvement.

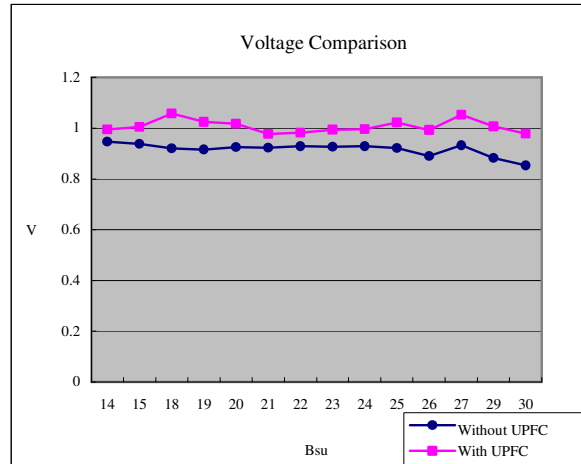


Fig. 5 Voltage comparison for 30% load

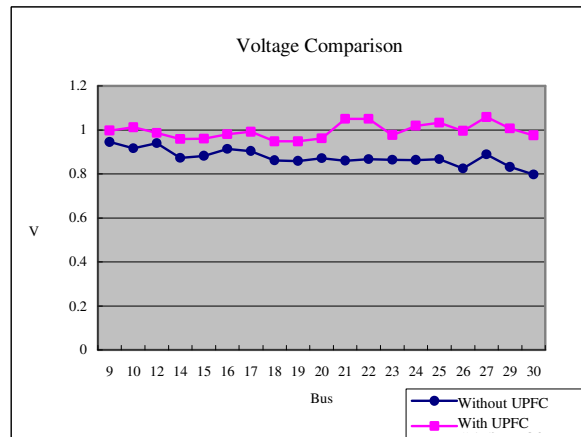


Fig. 6 Voltage comparison for 90% load

The results obtained by the different load conditions are shown in Table VI and Table VII. Fig. 6 and Fig. 7 illustrate the relationship between the different load conditions. From Table VI and Table VII, the capacity of the UPFC does change under different load condition.

TABLE VI  
LOCATION AND CAPACITY OF FIRST UPFC FOR DIFFERENT LOAD CONDITIONS

Load (%)	Location (Bus)	Capacity (MVA)
30	18	41.611
60	18	51.613
90	18	65.221

TABLE VII  
LOCATION AND CAPACITY OF SECOND UPFC FOR DIFFERENT LOAD CONDITIONS

Load (%)	Location (Bus)	Capacity (MVA)
30	27	22.729
60	27	24.165
90	27	25.265

## VI. CONCLUSIONS

The paper has demonstrated the application of MPSO for location and capacity of UPFC with ECI model in a power system considering at each bus the voltage constraints. The study is carried out for the aim of voltage security margin enhancement. Simulation results through an IEEE 30bus validate the efficiency of the optimal location and capacity of UPFC with the ECI model. The result shows the significantly voltage stability enhancement.

This paper presents a novel approach to OPF by using GA, and EP algorithms and enhancing the original PSO with adaptive velocity to the MPSO algorithm. The proposed approach utilizes the local and global capabilities to search for optimal cost reduction by OPF with UPFC. Compared with the results obtained by other methods in terms of solution quality, convergence rate and computation efficiency.

## ACKNOWLEDGMENT

The authors would like to acknowledge the financial support of the National Science Council of Taiwan, R.O.C. for this study through the grant: NSC 100-3113-P-110-003.

## REFERENCES

- [1] Abdel-Aty Edrisl, "FACTS technology development: an update," IEEE Power Engineering Review, vol.20, no.3, pp.4-9, Mar. 2000.
- [2] Sung-Hwan Song, Jung-Uk Lim, and sung-Il Moon, "FACTS Operation Scheme for Enhancement of Power System Security", Power Tech Conference Proceedings, Vol. 3, June 2003, pp. 36 – 41.
- [3] Y.D. Valle, J.C. Hernandez, G.K. Venayagamoorthy, R.G. Harley, "Multiple STATCOM Allocation and Sizing Using Particle Swarm Optimization", Power Systems Conference and Exposition, Oct. 2006, pp. 1884-1891.
- [4] Whei-Min Lin, Cong-Hui Huang, Tung-Sheng Zhan, "A Hybrid Current-Power Optimal Power Flow Technique", IEEE Transactions on Power System, Vol. 23, Feb. 2008, pp. 177-185
- [5] Y. del Valle, J.C. Hernandez, G.K. Venayagamoorthy, and R.G. Harley, "Optimal STATCOM Sizing and Placement Using Particle Swarn Optimization", Transmission & Distribution Conference, Latin America, Aug. 2006, pp.1-6.
- [6] N. Boonpirom, K. Paitoonwattanakij, "Static Voltage Stability Enhancement using FACTS", The 7th International Power Engineering Conference, Vol. 2, Dec 2005, pp. 711 – 715.
- [7] W. M. Lin, Y. S. Su, H. C. Chin, and J. H. Teng, "Three-Phase Unbalanced Distribution Power Flow Solutions with Minimum Data Preparation," *IEEE Transactions on power Systems*, vol. 143, pp. 1178-1183, Aug. 1999.
- [8] W. M. Lin, T. S. Zhan, and M. T. Tsay, "Multiple-frequency threephase load flow for harmonic analysis," *IEEE Trans. Power Syst.*, vol. 19, no. 2, pp. 897-904, May 2004.
- [9] M. A. Abido, "Optimal power flow using particle swarm optimization," *Electrical Power and Energy Systems*, vol. 24, pp. 563-571, 2002.